Distributed Batteryless Access Control for Data and Energy Integrated Networks: Modeling and Performance Analysis

Xinyu Fan, Jie Hu, *Senior Member, IEEE*, Yizhe Zhao, *Member, IEEE*, Kun Yang, *Fellow, IEEE*

***Abstract*—Radio-frequency (RF) signals are capable of simultaneously transferring data and energy from a hybrid access point (HAP) toward battery-powered and batteryless wireless devices. Battery-powered and batteryless wireless devices with the capability of RF energy harvesting need a distributed access control protocol with collision avoidance to achieve higher energy efficiency. We study the performance of a data and energy integrated network (DEIN) that adopts an enhanced carrier sensing multiple access with collision avoidance (CSMA/CA) protocol. Each device in this network can switch to RF energy harvesting mode or data reception mode according to HAP's instruction, and freezes its backoff counter when energy storage is insufficient. By invoking a three-dimensional (3D) Markov chain, we model the operating behaviors of batteryless wireless devices and an HAP in a DEIN. Apart from backoff operations of devices, the 3D Markov chain also depicts their dynamic energy changes, including RF energy harvesting and energy consumption. Wireless devices consume energy harvested from the HAP's downlink transmissions for powering their data upload and random backoff. With the aid of the 3D Markov chain, the upload throughput of devices can be obtained in semi-closed-form. Moreover, a decoupling method is proposed to approximate throughput performance with low complexity. The accuracy of our theoretical model is validated by simulation results. By characterizing the impact of various parameters on throughput performance, a design guideline for a DEIN with a distributed batteryless access protocol is provided.**

***Index Terms*—energy sustainability, simultaneous wireless information and power transfer, batteryless wireless devices, distributed batteryless access control, throughput analysis, Markov chain.**

Manuscript received November 12, 2022; revised January 09, 2023 and February 09, 2023; accepted March 24, 2023. This paper was partly funded by Natural Science Foundation of China (No. 62132004, 61971102, 62201123), MOST Major Research and Development Project (No. 2021YFB2900204), Sichuan Science and Technology Program (No. 2022YFH0022 and 22QYCX0168), UESTC Yangtze Delta Region Research Institute-Quzhou (No. 2022D031), China Postdoctoral Science Foundation (Grant No. 2022TQ0056), and EU H2020 Project COSAFE (GA-824019).

Xinyu Fan, Jie Hu and Yizhe Zhao are with the School of Information and Communication Engineering, University of Electronic Science and Technology of China, Chengdu, 611731, China, email: xinyu_fan@std.uestc.edu.cn, hujie@uestc.edu.cn, and yzzhao@uestc.edu.cn

Kun Yang is with the School of Information and Communication Engineering, University of Electronic Science and Technology of China, Chengdu, 611731, China, and also with the School of Computer Science and Electronic Engineering, University of Essex, Colchester, CO4 3SQ, U.K., email: kunyang@essex.ac.uk.

I. Introduction

A. Background and Motivation

Many Internet of Everything (IoE) devices are powered by embedded batteries with limited capacity. In order to maintain their regular operations, these batteries have to be frequently replaced, which substantially increases network maintenance cost. Harvesting energy from radio frequency (RF) signals [1], [2] is capable of prolonging the lifetime of wireless devices. Different from uncontrollable ambient energy harvesting [3]–[6], RF energy harvesting can be controlled by allowing base stations (BSs) and access points (APs) to actively emit RF signals, which is regarded as RF signal based wireless energy transfer (WET). Coordinating traditional wireless data transfer (WDT) together with wireless energy transfer yields a novel data and energy integrated network (DEIN) [7]. This is a promising technique to achieve energy sustainability in future 6G [8]. One of the typical applications of DEIN is to provide far-field recharging and communications services in wireless sensor networks [9].

In a DEIN [7], wireless devices can harvest RF energy from transmitters and thus achieve a longer lifetime. Many works focus on improving the efficiency of wireless data and energy transfer in DEIN from a physical layer aspect. For example, Clerckx *et al*. [10] designed optimal waveform to improve the efficiency of wireless energy transfer. Moreover, many works analyzed the network performance of DEIN [11], [12]. Lu *et al*. [11] analyzed the energy outage probability of a wireless device in a DEIN, where RF transmitters were distributed by following a Ginibre point process. Liu *et al.* [12] studied the impact of network deployment on the average power harvested by wireless devices in a multi-tier heterogeneous DEIN. However, the above-mentioned works did not consider the impact of devices' access behaviors on the probabilities of energy transmitters transmitting RF energy, which further affect devices' RF energy harvesting performance. Moreover, access behaviors directly affect how much energy is consumed by wireless devices for data transmission, data reception, sleeping, and some other necessary operations. Therefore, access control protocols of battery-powered and batteryless wireless devices should be carefully considered for achieving energy-sustainability in DEINs [13]. Moreover, we need accurate theoretical performance analysis in network planning stage of DEIN, before it can be practically deployed. Otherwise, engineers have to rely on time-consuming Monte-Carlo simulation for estimating network performance. Bianchi [14]

first proposed a Markov chain based framework for analyzing the performance of a CSMA/CA protocol, which stimulated wide interest in relevant research. However, Bianchi's analytical modeling is only suitable for wireless devices with sufficient energy storage. In line with this motivation, our paper aims to study the effect of access control behaviors on the performance of battery-powered and batteryless wireless devices in a DEIN system, while analyzing its performance in semi-closed-form.

B. Related Works

Centrally controlled access protocols have been widely adopted in DEINs [15], [16], in which central controllers may allocate orthogonal time or frequency resources to wireless devices based on their channel state information and their status reported. However, centrally controlled protocols require frequent information exchange between wireless devices and central controllers for time synchronization, channel state information feedback and resource allocation results. This may quickly consume the limited energy storage of wireless devices.

Apart from centrally controlled networks, such as cellular networks, many devices access the network for wireless data transfer in a distributed manner [17], [18]. Specifically, Liang *et al*. [17] proposed a duty-cycle based access control protocol to achieve low latency for wireless devices by adjusting sleep windows. Zhi *et al*. [18] proposed a probabilistic polling based random access protocol for multi-hop RF energy harvesting aided wireless sensor networks. However, these random access protocols did not consider collision avoidance, which made wireless devices consume more energy for frequent retransmission. Their limited energy storage might be quickly drained.

The classic CSMA/CA protocol effectively reduces collision probabilities. Each device with a transmission request has to wait for a random period to avoid any collision. The length of this random waiting period is determined by backoff counter. The distributed and collision avoidance characteristics of CSMA/CA make it suited for battery-powered and batteryless devices. Based on Bianchi's [14] analysis framework, many works studied CSMA/CA based access control protocols for different networks with a Markov chain [19]–[22]. Specifically, Li *et al*. [19], [20] proposed a CSMA/CA based protocol for an air-ground integration network. They divided ground devices in the coverage into different clusters according to their communication duration. A 3D Markov chain was exploited to model backoff stages, the backoff counters, and the number of clusters. Li *et al*. [21] studied a block access control protocol in a blockchain-based wireless local-area network (B-WLAN). Moreover, Choi *et al*. [22] designed a contention window control scheme for the CSMA/CA protocol, while they analyzed its performance in terms of the collision probability, collision time, and backoff time. Unfortunately, these works only study the wireless devices which always have sufficient energy to support their operations, while totally ignoring either their practical energy consumption or their energy harvesting.

The CSMA/CA protocol was adopted for wireless devices enabled by RF energy harvesting capabilities [23], [24]. Naderi *et al*. [23] studied an enhanced CSMA/CA protocol named RF-MAC to optimize the energy delivery of wireless devices. Wireless devices could actively request energy from HAP. By responding to these requests, HAP recharged these wireless devices on demand. Based on RF-MAC, Tamilarasi *et al*. [24] studied a DEIN system that allocated the same rate to all wireless devices regardless of their different channel states. However, they did not consider theoretical analysis, all performances were derived by time-consuming Monte-Carlo simulation.

The Bianchi [14]'s Markov chain based analysis framework was also adopted for modeling the behaviors of wireless devices enabled by RF energy harvesting capabilities [25]–[28]. Specifically, Arshad *et al*. [25] studied a wireless powered communication network assisted by a relay, where the relay transmitted both wireless data and energy to wireless devices. A 2D Markov chain was relied upon for modeling a distributed access control protocol of wireless devices. However, the energy storage of devices was inaccurately simplified as several discrete states, while the zero-energy state was completely ignored. In practice, a batteryless wireless device inevitably depletes its limited energy storage. In this situation, it cannot transmit any data packets or take any backoff operations, which further reduces its throughput performance. In this state, wireless devices cannot transmit or backoff, which further affects throughput performance. Khairy *et al*. [26] studied the AP's beacon frequency and the recharging period of wireless devices in WiFi based on Bianchi's analytical results. However, battery-powered and batteryless wireless devices suffer both collision and energy insufficient problems, which further affect the data transmission performance of devices. Therefore, Bianchi's analytical modeling is only suitable for wireless devices with sufficient energy storage. In [27], [28], the throughput performance of a CSMA/CA protocol based network with batteryless wireless devices was analyzed with an incomplete energy consumption model. Only the energy consumption for data upload was considered, while the energy consumption for the random backoff process was totally ignored. Moreover, they impractically assume that a wireless device depleted all its energy storage for uploading a single data packet.

C. Novel contributions

Against the drawbacks we mentioned above, we considered a DEIN system with an RF energy harvesting enhanced CSMA/CA protocol, and further analyze the performance of batteryless devices with this protocol. To the best of our knowledge, no studies accurately characterize dynamic energy states and the wireless data transfer process of a batteryless wireless device with a distributed access control protocol. The main contributions are summarized as follows:

- We analyze the performance of wireless devices with an RF energy harvesting enhanced CSMA/CA protocol in a DEIN, where each device may switch to RF energy harvesting mode or data reception mode according to HAP's instruction and freeze its backoff counter when its energy storage is insufficient. All these devices' data

uploading is powered by energy harvested from the downlink transmission of the HAP.

- A 3D Markov chain is exploited to model the operations of wireless devices. This 3D Markov chain accurately characterizes RF energy harvesting of wireless devices, and their energy consumption for data upload and for collision avoidance oriented backoff process, which is never considered in existing works.
- In order to reduce the complexity, the 3D Markov chain is decoupled in the data-domain and the energy-domain which help us derive approximated access probabilities and the throughput performance of both the HAP and devices in semi-closed-form.

The rest of this paper is organized as follows. After introducing the system model in Section II, our 3D Markov chain based modeling and the theoretical analysis are described in Section III. We then provide simulation results in Section IV, before we finally conclude in Section V. Unless specified, battery-powered and batteryless wireless devices are referred to as devices in the rest of this paper.

II. Batteryless distributed access control protocol

A. System model

As shown in Fig. 1, our DEIN system consists of a single HAP with a stable energy source, and N batteryless wireless devices (WD), which are indexed by an integer $\mu \in \{0, 1, \ldots, N\}$. Wireless devices are randomly deployed around the HAP, and the distance between WD_μ and HAP is d_μ. Note that all devices are equipped with supercapacitors for energy storage. Wireless devices can only communicate with the HAP. Direct communications among themselves are not allowed. All devices and HAP are equipped with a single antenna. HAP always transmits with its maximum transmit power P_{AP}, and the WD_μ's transmit power depends on its distance to the HAP. The physical layer model and MAC layer model of the system are separately described in the following subsections.

The channel model is constituted by a distance-dependent path-loss and an additional random term ζ_μ accounting for small-scale fading. A similar channel model is used in [29]. The instantaneous channel power gain between the HAP and the WD_μ can be then expressed as

$$h_\mu = G_R G_T (\frac{c}{4\pi f_0 d_0})^2 (\frac{d_0}{d_\mu})^\beta \zeta_\mu, \tag{1}$$

where G_T and G_R are the transmit and receive antennas' gains, c is the speed of the light and β is the path-loss exponent. Moreover, in Eq. (1), f_0 is the carrier frequency. Furthermore, d_0 represents the near-field range of the HAP. $\zeta_\mu \sim \text{Exp}(1)$ is an exponential random variable with unit mean accounting for small-scale Rayleigh fading. Due to the duration of the require to send (RTS) and clear to send (CTS) packets is very small, the HAP can only transfer sufficient energy toward devices during the data packet transmissions. We consider the device as a time switching RF energy harvesting receiver [7]. When the device is harvesting energy, it will not receive any packets. The duration of the data packet transmission is denoted as T_{PCK}. By considering a non-linear energy harvesting model [30], [31], the energy harvested by WD_μ can be expressed as

$$E_\mu^H = \left[\frac{P_{max}}{\exp(-AP_0 + B)} (\frac{1 + \exp(-AP_0 + B)}{1 + \exp(-AP_{\text{AP}} \overline{h}_\mu + B)} - 1) \right] \text{T}_{\text{PCK}}, \tag{2}$$

where $\overline{h}_\mu = \mathbf{E}[h_\mu]$ is the average channel power gain; P_{max} is the maximum harvestable power when RF energy harvesting circuit is saturated; P_0 is the harvester's sensitivity threshold; A and B are both constants related to the RF energy harvesting circuit's resistance, capacitance and diode's turn-on voltage.

Let us now consider the data packet uploading of WD_μ. Only when the signal-to-noise-ratio (SNR) is higher than a predefined threshold γ_{th}, the data packet transmitted from WD_μ can be correctly decoded by the HAP. We denote the energy consumption of WD_μ for its data packet transmission E_μ^{PCK}, which should satisfy the following outage constraint as:

$$P_r \left(\frac{E_\mu^{\text{PCK}} h_\mu}{B N_0 \text{T}_{\text{PCK}}} \leq \gamma_{\text{th}} \right) \leq \xi, \tag{3}$$

where B is bandwidth, N_0 is the power spectral density of the additive white Gaussian noise (AWGN), and ξ is the symbol error rate (SER) threshold which the outage probability should satisfy. Therefore, by solving Eq. (3), E_μ^{PCK} can be obtained as

$$E_\mu^{\text{PCK}} = \frac{B N_0 \text{T}_{\text{PCK}} \gamma_{\text{th}}}{F_{h_\mu}^{-1}(\xi)}, \tag{4}$$

where $F_{h_\mu}^{-1}(.)$ represents the inverse cumulative distribution function of the channel power coefficient h_μ. Note that Eq. (4) is used for deriving the energy consumption of data packet transmission. By considering path-loss, a device with data transmission requests chooses a proper transmit power to ensure that all data packets can be successfully transmitted in uplink. HAP always transmits with its maximum power P_{AP}, which also results in a zero packet loss rate in the downlink data packet transmission.

B. Protocol description

All wireless devices and the HAP operate at the same frequency, only one device (or HAP) is allowed to transmit at the same time. When a device gains the highest priority to access the channel, it also has to have sufficient energy for powering its data transmission. The general operation of a device in this protocol is summarized as the following steps:

- *Step 1*: A device with data packets to be transmitted senses the channel.
- *Step 2*: When the channel is free, the device initializes its backoff stage as $i = 0$. It also initializes the backoff counter as a random number within $[0, W_0 - 1]$, where W_0 represents the initial backoff window size.
- *Step 3*: The backoff counter reduces by one during every backoff interval, if the channel is still free. Otherwise, the device freezes its backoff counter. Moreover, the device continuously consumes energy during the backoff process. If the energy storage of the device is not sufficient

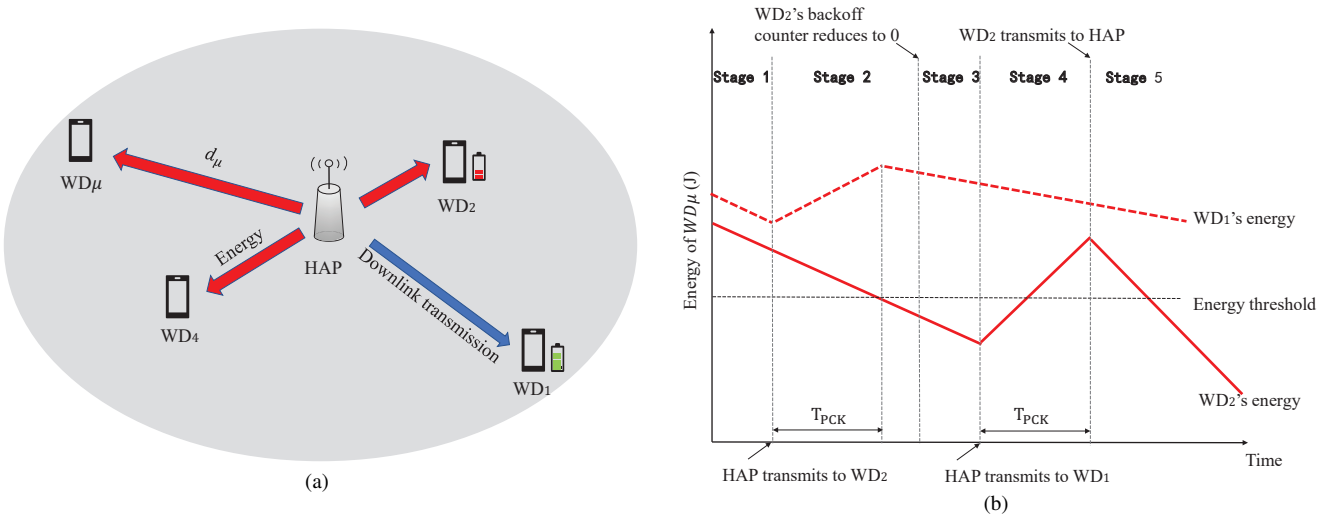

Fig. 1. System model and an example for the energy dynamics of batteryless wireless devices

for backoff, it freezes the backoff counter until sufficient energy is harvested.

- *Step 4*: After the backoff counter reduces to zero, it starts its RTS/CTS handshake for data packet transmissions if it has gained sufficient energy for data packet transmissions.
- *Step 5*: If the transmission suffers from a collision, the device then increases the backoff stage to $i = i + 1$, while initializing the backoff counter as a random number within $[0, W_i - 1]$, where we have $W_i = 2W_{i-1}$.
- *Step 6*: When the device receives an RTS packet from the HAP, it switches to data packet reception mode if it is the destination of this RTS packet. Otherwise, it switches to the RF energy harvesting mode. It then switches back to the data packet reception mode, once the HAP finishes its data packet transmission.

Moreover, when the HAP transmits data packets toward a device, the other devices harvest energy carried by downlink RF signals. The energy harvested can be obtained by Eq. (2). A device can operate either in a data packet reception mode or in an RF energy harvesting mode in a time switching manner. The RTS packet can also be regarded as a mode-switching instruction. When WD_μ receives an RTS packet from HAP, it switches to the RF energy harvesting mode, if it is not the destination of this RTS packet. Otherwise, it switches to the data packet reception mode instead. Only when the received RF power satisfies the threshold of the device's energy harvester, can the device convert the RF energy into DC energy. We assume that devices can only harvest energy from the downlink transmission of the HAP, they cannot harvest energy from their peers.

We also exemplify the energy dynamics of the devices with our distributed batteryless access control protocol in Fig. 1 (b), where we have a single HAP and two devices. Fig. 1 is a simplified schematic diagram, that we do not consider a realistic model for energy harvesting and energy consumption. The duration of each Stage is also not proportional in Fig. 1. During Stage 1, the channel is free, all devices are taking backoff operations, and continuously consume energy for backoff and channel estimation. At the end of Stage 1, the HAP's backoff counter first reduces to zero. It then starts to communicate with WD_2 after the RTS/CTS handshaking. During Stage 2, WD_1 switches to the RF energy harvesting mode and harvests energy from the downlink transmission of the HAP to replenish its energy storage, while WD_2's energy storage reduces for powering its own data packet reception. Note that WD_2 cannot harvest energy at this stage because it switches to the data packet reception mode rather than the RF energy harvesting mode. After a duration of T_{PCK}, all devices restart their backoff process. At the end of Stage 2, although WD_2's backoff counter reduces to zero, it cannot transmit any data packet because its energy storage is lower than the minimum requirement for data packet uploading. Then after several backoff intervals, the HAP also has a zero backoff counter, and it is allowed for downlink data packet transmissions. During Stage 4, WD_2 may harvest energy, while WD_1 consumes its energy storage for data packet reception. As shown in Fig. 1, at the end of Stage 4, WD_2 harvests sufficient energy to support its data packet uploading. Since its backoff counter is zero, it can immediately commence the data packet uploading process during Stage 5, which may consume the amount E_{PCK} of WD_2's energy storage. Observe from Fig. 1 that, WD_1 cannot harvest energy during Stage 5, when WD_2 uploads its data packet. Therefore, WD_1 only consumes energy for the backoff process.

III. Modeling and Throughput Analysis

All devices and the HAP are assumed to have full buffers. Therefore, they always have data packets pending to be transmitted. Moreover, the HAP has equal probabilities to transmit data packets to all devices. Under this assumption, we derive all the upper-bounded system performance of the distributed batteryless access control protocol.

A. 3D Markov Modeling

In order to obtain the transmission probabilities of the devices and the HAP, a specific device's operational behaviors

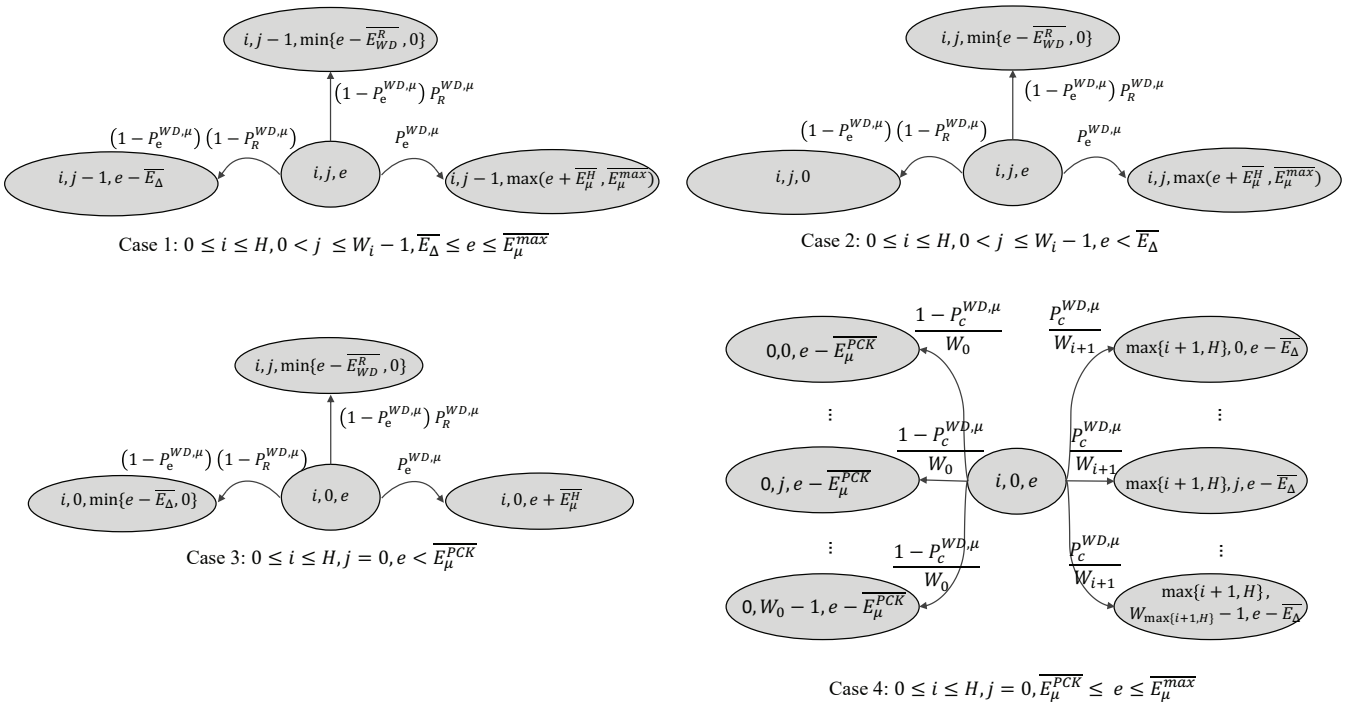

Fig. 2. 3D Markov chain model of WD_μ

can be modeled as a discrete 3D Markov chain, as shown in Fig. 2. A tuple $[s(t), c(t), e(t)]$ with three elements defines the state of a device during the t-th time slot. Specifically, $s(t) = i \in [0, H]$ represents the backoff stage, $c(t) = j \in [0, W_i - 1]$ represents the backoff counter, while $e(t) = e \in [0, \overline{E}_\mu^{\max}]$ represents the energy state of WD_μ. Actually, the length of a time slot is not a fixed value and is related to WD_μ's operations, which include successful transmission, transmission collision, and no transmission. We denote the length of a time slot in these three operations as T_s, T_c, and T_f, respectively. When WD_μ does not transmit any data packets (no transmission), it may take a backoff operation, or take none operation if it does not have any energy storage. Moreover, we denote the average length of a time slot as $\mathbf{E}[\textit{time-slot}]$. We introduce a discrete energy unit E_δ. A positive integer $\overline{E}_\mu^{\max} = Q/E_\delta$ is defined as the maximum discrete energy capacity, where Q is the actual capacity of the energy storage. The discrete energy threshold for data packet transmissions can be expressed as $\overline{E_\mu}^{\mathrm{PCK}} = \lceil E_\mu^{\mathrm{PCK}}/E_\delta \rceil$, while the discrete energy harvested by WD_μ can be expressed as $\overline{E_\mu}^{H} = \lceil E_\mu^{H}/E_\delta \rceil$. We denote the average energy consumption of the backoff operation and channel detection operation of WD_μ in a transmission frame as E_Δ. Its discrete version can be expressed as $\overline{E}_\Delta = \lceil E_\Delta/E_\delta \rceil$. Moreover, when a device receives a packet from HAP, we denote that it will consume E_{WD}^R energy, which should be proportional to the length of $\mathrm{T_{PCK}}$, and its discrete version is expressed as $\overline{E}_{\mathrm{WD}}^R = \lceil E_{\mathrm{WD}}^R/E_\delta \rceil$. The probability of a device harvesting energy when it is not transmitting packets is denoted as $P_e^{\mathrm{WD},\mu}$. If a device has sufficient energy storage and its backoff counter reduces to zero, it may send an RTS packet to the HAP. However, concurrent transmission attempts of multiple devices may induce collisions. We denote the probability of transmission collisions when WD_μ transmits a packet as $P_c^{\mathrm{WD},\mu}$. When WD_μ is not transmitting, the probability of WD_μ receiving a packet from the HAP is denoted as $P_R^{\mathrm{WD},\mu}$. Note that $P_c^{\mathrm{WD},\mu}$, $P_e^{\mathrm{WD},\mu}$ and $P_R^{\mathrm{WD},\mu}$ can be calculated in Section III-D. Moreover, all these probabilities of WD_μ are jointly determined by the behaviors of the other devices and the HAP. Therefore, they are independent of the device's own states. The main notations used are given in TABLE I.

When the backoff counter j of WD_μ does not reduce to zero, it cannot transmit any data packets, as shown in Cases 1-2 of Fig. 2. Specifically, in Case 1 of $0 \le i \le H$, $0 < j \le W_i - 1$, and $\overline{E}_\Delta \le e \le \overline{E}_\mu^{\max}$, WD_μ's backoff counter j reduces by one. It may either harvest $\overline{E_\mu}^{H}$ energy with a probability of $P_e^{\mathrm{WD},\mu}$ or consume energy for data reception or backoff operation. The HAP may choose WD_μ as the packet destination. Therefore, WD_μ may consume $\overline{E}_{\mathrm{WD}}^R$ energy with a probability of $(1 - P_e^{\mathrm{WD},\mu})P_R^{\mathrm{WD},\mu}$. If the HAP may not choose WD_μ as the packet destination, WD_μ may consume $\overline{E}_\Delta$ energy for backoff operation with a probability of $(1 - P_e^{\mathrm{WD},\mu})(1 - P_R^{\mathrm{WD},\mu})$. Moreover, the energy state e of WD_μ can only transit to zero, when WD_μ does not have sufficient energy to consume. In Case 2 of $e < \overline{E}_\Delta$, the WD_μ freezes its backoff counter because its energy is exhausted. The transition duration of each state is T_s, when WD_μ harvests energy or receives a packet. It is T_f, when WD_μ only takes a single backoff operation.

When the backoff counter j reduces to 0, WD_μ still cannot transmit any data packets with insufficient energy storage, as shown in Cases 3 of Fig. 2. Normally, data packet transmis-

TABLE I
MATHEMATICAL NOTATIONS AND ABBREVIATIONS

Notation	Description	Notation	Description
HAP	Hybrid access point	WD	Wireless device
WET	Wireless energy transfer	WDT	Wireless data transfer
RTS	Require to send	CTS	Clear to send
N	Number of wireless devices	d_μ	Distance between HAP and WD_μ (m)
T_{PCK}	Duration of a packet	P_{AP}	Transmit power of the AP
$P_{\max}$	Maximum harvestable power	P_0	Energy harvester's sensitivity threshold
E_μ^H,$\overline{E_\mu}^H$	Energy harvested by WD_μ	E_μ^{PCK},$\overline{E_\mu}^{\text{PCK}}$	Energy consumed for a packet transmission
E_δ	Discrete energy unit	E_{WD}^R,E_{AP}^R	Energy consumed for a packet reception
Q,$\overline{E}_\mu^{\max}$	Maximum energy of capacitance	E_Δ,$\overline{E}_\Delta$	Energy consumed for backoff operation and channel detection
T_s,T_c	Length of a time slot, when channel is occupied by a successful transmission or a collision.	H,W_0	Maximum backoff stage and initial backoff window size
T_f	Length of a time slot, when channel is free	$P_c^{\text{WD},\mu}$	Collision probability of WD_μ
$P_R^{\text{WD},\mu}$	Data reception probability of WD_μ	$P_e^{\text{WD},\mu}$	Energy harvesting probability of WD_μ
$b_n^{\text{WD},\mu}$	Probability of WD_μ does not have enough energy for backoff	$b_e^{\text{WD},\mu}$	Probability of WD_μ has enough energy for data transmission
$b_s^{\text{WD},\mu}$	Probability of WD_μ has a successful transmission	$\tau^{\text{WD},\mu}$,τ^{AP}	WD_μ and HAP's transmission probability
P_c^{AP}	Collision probability of HAP	P_s^{AP},P_s^{WD},P_f	Probabilities of channel is occupied by HAP or device's successful transmission, and probability of channel is free
$R_{downlink}$,R_{uplink}	Downlink and uplink throughput	P_{Totol}	Power consumed by HAP

sions have a longer duration T_{PCK} than the backoff intervals. Therefore, the energy consumption $\overline{E_\mu}^{\text{PCK}}$ is higher than $\overline{E}_\Delta$. Moreover, due to the path-loss of RF signals' propagation, the energy harvested by WD_μ should be much lower than E_μ^{max}. Without loss of generality, we assume $\overline{E_\mu}^{\text{PCK}} + \overline{E_\mu}^H < \overline{E}_\mu^{\max}$. Therefore, in Case 3 of $0 \le i \le H$, $j = 0$, and $e < \overline{E_\mu}^{\text{PCK}}$, WD_μ cannot transmit any data packets. We should consider the following three situations: 1) It may harvest $\overline{E_\mu}^H$ energy with a probability of $P_e^{\text{WD},\mu}$; 2) It consumes $\overline{E}_\Delta$ energy with a probability of $(1 - P_e^{\text{WD},\mu})(1 - P_R^{\text{WD},\mu})$; 3) It may consume $\overline{E}_{\text{WD}}^R$ energy with a probability of $(1-P_e^{\text{WD},\mu})P_R^{\text{WD},\mu}$. Moreover, the energy storage e of WD_μ can only reduce to 0 without harvesting any energy, when $e < \overline{E}_\Delta$. The transition duration of each state is T_s, when WD_μ harvests energy or receives a packet, while it is T_f when WD_μ only takes a single backoff operation.

When the backoff counter j reduces to 0 and WD_μ's energy storage is higher than E_μ^{PCK}, WD_μ transmits data packets in Cases 3 of Fig. 2. When no collision happens with a probability of $(1 - P_c^{\text{WD},\mu})$, WD_μ sets its backoff stage i to 0 and initializes its backoff counter j to a random number within $[0, W_0 - 1]$. WD_μ then consumes $\overline{E_\mu}^{\text{PCK}}$ energy for a data packet transmission. When the collision happens with a probability of $P_c^{\text{WD},\mu}$, WD_μ increases its backoff stage i by one, and chooses a random number within the range of $[0, W_{i+1} - 1]$ as its backoff counter j. It then consumes $\overline{E}_\Delta$ energy for the backoff process. When the backoff stage reaches the maximum H, it may not increase anymore. The transition duration of each state is T_s, when no collision happens, otherwise, it is T_c.

Observe from Fig. 2 that the transition probabilities between every pair of states in the 3D Markov chain are related to the collision probability $P_c^{\text{WD},\mu}$, reception probability $P_R^{\text{WD},\mu}$ and energy harvesting probability $P_e^{\text{WD},\mu}$. Therefore, the stationary probabilities of the 3D Markov chain are determined by $P_c^{\text{WD},\mu}$ $P_R^{\text{WD},\mu}$and $P_e^{\text{WD},\mu}$. Moreover, these probabilities are also determined by the stationary probabilities and vice versa. In order to calculate $P_c^{\text{WD},\mu}$, $P_R^{\text{WD},\mu}$, $P_e^{\text{WD},\mu}$ and all the stationary probabilities, we first fix $P_c^{\text{WD},\mu}$, $P_R^{\text{WD},\mu}$ and $P_e^{\text{WD},\mu}$ to calculate the stationary probabilities and then use the calculated stationary probabilities to update $P_c^{\text{WD},\mu}$, $P_R^{\text{WD},\mu}$ and $P_e^{\text{WD},\mu}$. However, the 3D Markov chain has $\overline{E}_\mu^{\max} W_0(2^{H+1} - 1)$ states. The stationary probabilities can be denoted as an $\overline{E}_\mu^{\max} W_0(2^{H+1} - 1) \times 1$ vector $\mathbf{\Pi}$. The state transition probabilities can be denoted as an $\overline{E}_\mu^{\max} W_0(2^{H+1} - 1) \times \overline{E}_\mu^{\max} W_0(2^{H+1} - 1)$ matrix $\mathbf{P}$ which can be derived by Fig. 2. $\mathbf{\Pi}$ can be obtained by solving the following equations:

$$\begin{cases} \mathbf{\Pi P} = \mathbf{\Pi}, \\ \sum \mathbf{\Pi} = 1. \end{cases} \tag{5}$$

The complexity for solving Eq. (5) is $\mathcal{O}((\overline{E}_\mu^{max} W(2^{H+1} - 1)^3))$. In order to reduce the complexity, the original 3D Markov chain is decoupled into an independent 2D counterpart for characterizing WD_μ's behavior in the data packet transmission and an independent 1D counterpart for reflecting WD_μ's dynamic energy storage.

B. Analysis in the data packet transmission

The state of WD_μ is represented by $[s(t) = i, c(t) = j]$ in the data packet transmission domain. Apart from the transmission collision probability $P_c^{\text{WD},\mu}$, we denote the probability of WD_μ having no energy at all as $b_n^{\text{WD},\mu}$, while denoting the probability of the WD_μ having sufficient energy for data packet transmissions as $b_e^{\text{WD},\mu}$. Furthermore, the probability of the WD_μ having sufficient energy for data packet receptions is denoted as $b_r^{\text{WD},\mu}$.

As depicted in Fig. 3, in the case of $0 \le i \le H$ and $j > 0$, the backoff counter continues to reduce by one, if WD_μ has

some energy with a probability of $(1-b_n^{\mathrm{WD},\mu})$. WD_μ's state may transit to $[s(t), c(t)-1]$ from $[s(t), c(t)]$. By contrast, WD_μ freezes its backoff counter if it does not have any energy with a probability of $b_n^{\mathrm{WD},\mu}$. WD_μ may maintain its current state $[s(t), c(t)]$.

When the backoff counter reduces to zero, WD_μ is ready for data packet transmission. If it has sufficient energy and no collision happens, the data packet transmission is successful. WD_μ then sets its backoff stage to zero, while choosing a random number within the range of $[0, W_0-1]$ as its backoff counter. As depicted in Fig. 3, in the case of $0 \le i \le H$ and $j=0$, the probability of a device successfully transmitting a data packet can be formulated as $b_e^{\mathrm{WD},\mu}(1-P_c^{\mathrm{WD},\mu})$. WD_μ's state may transit to $[s(t)=0, c(t)=j]$ from $[s(t), c(t)=0]$, while j is a random number uniformly chosen from $[0, W_0-1]$. Since WD_μ uniformly chooses a number as its backoff counter, the state transition to every $[s(t)=0, c(t)=j]$ for $\forall j \in [0, W_0-1]$ has the same probability of $\frac{b_e^{\mathrm{WD},\mu}(1-P_c^{\mathrm{WD},\mu})}{W_0}$.

By contrast, if the data packet transmission fails, WD_μ increases its backoff stage by one and chooses a random number within the range of $[0, W_i-1]$ as its backoff counter. As depicted in Fig. 3, in the case of $0 \le i < H$ and $j=0$, the probability that a device has sufficient energy but some collisions happen can be formulated as $b_e^{\mathrm{WD},\mu}P_c^{\mathrm{WD},\mu}$. Similarly, since the backoff counter j is uniformly chosen, WD_μ's state may transit to $[s(t)=i+1, c(t)=j]$ from $[s(t)=i, c(t)=0]$ with the same probability of $\frac{b_e^{\mathrm{WD},\mu}P_c^{\mathrm{WD},\mu}}{W_i}$. When the backoff stage reaches the maximum H, it may not increase anymore. In the case of $i=H$ and $j=0$ as shown in Fig. 3, WD_μ's state may transit to $[s(t)=H, 0 \le c(t)=j \le W_H-1]$ from $[s(t)=H, c(t)=0]$ with the same probability of $\frac{b_e^{\mathrm{WD},\mu}P_c^{\mathrm{WD},\mu}}{W_H}$.

If WD_μ does not have sufficient energy, when the backoff counter reduces to zero, it maintains its backoff stage. As depicted in Fig. 3, in the case of $0 \le i \le H$ and $j=0$, WD_μ may maintain its state $[s(t)=i, c(t)=0]$ with a probability of $(1-b_e^{\mathrm{WD},\mu})$.

We denote the stationary probabilities of the 2D Markov chain in the data packet transmission domain as $\{\pi_{i,j}^D | \forall i = s(t), j = e(t)\}$. According to Fig. 3, these stationary probabilities obey the following equations:

$$\begin{cases} \pi_{i,0}^D = \pi_{i,0}^D(1-b_e^{\mathrm{WD},\mu}) + \sum_{j=0}^{W_i-1} \pi_{i-1,0}^D \frac{b_e^{\mathrm{WD},\mu}P_c^{\mathrm{WD},\mu}}{W_i}(1-b_n^{\mathrm{WD},\mu})^j, \\ \qquad\qquad 1 \le i \le H-1, \\ \pi_{H,0}^D = \pi_{H,0}^D(1-b_e^{\mathrm{WD},\mu}) + \sum_{j=0}^{W_H-1} \pi_{H-1,0}^D \frac{b_e^{\mathrm{WD},\mu}P_c^{\mathrm{WD},\mu}}{W_H}(1-b_n^{\mathrm{WD},\mu})^j \\ \qquad + \sum_{j=0}^{W_H-1} \pi_{H,0}^D \frac{b_e^{\mathrm{WD},\mu}P_c^{\mathrm{WD},\mu}}{W_H}(1-b_n^{\mathrm{WD},\mu})^j, \\ \qquad\qquad i = H. \end{cases} \tag{6}$$

Eq. (6) can be further simplified as

$$\begin{cases} \pi_{i,0}^D = \sum_{j=0}^{W_i-1} \pi_{i-1,0}^D \frac{P_c^{\mathrm{WD},\mu}}{W_i}(1-b_n^{\mathrm{WD},\mu})^j, \qquad 1 \le i \le H-1, \\ \pi_{H,0}^D = \sum_{j=0}^{W_H-1} \pi_{H-1,0}^D \frac{P_c^{\mathrm{WD},\mu}}{W_H}(1-b_n^{\mathrm{WD},\mu})^j \\ \qquad + \sum_{j=0}^{W_H-1} \pi_{H,0}^D \frac{P_c^{\mathrm{WD},\mu}}{W_H}(1-b_n^{\mathrm{WD},\mu})^j, \qquad i = H. \end{cases} \tag{7}$$

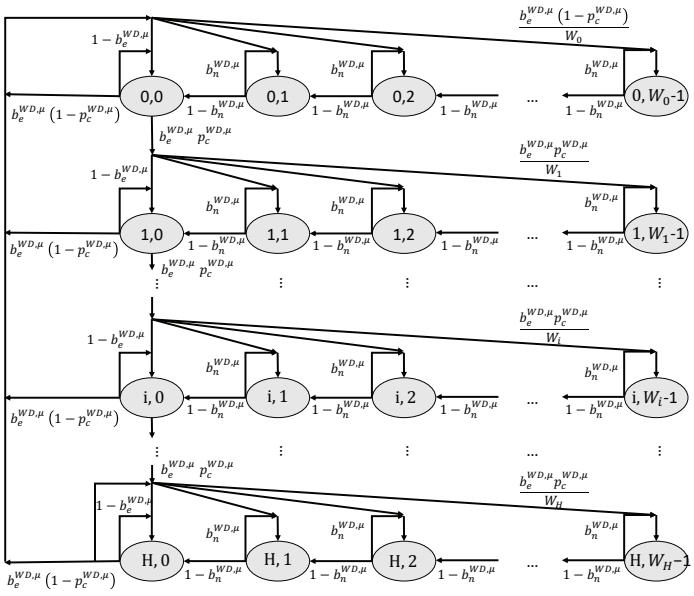

Fig. 3. 2D Markov chain in the data transmission domain.

By recursively solving Eq. (7), we may derive

$$\begin{cases} \pi_{i,0}^D = \pi_{0,0}^D \prod_{m=1}^{i} \sum_{j=0}^{W_m-1} \frac{P_c^{\mathrm{WD},\mu}}{W_m}(1-b_n^{\mathrm{WD},\mu})^j, \\ \qquad\qquad 1 \le i \le H-1. \\ \pi_{H,0}^D = \frac{\pi_{H-1,0}^D \sum_{j=0}^{W_H-1} \frac{P_c^{\mathrm{WD},\mu}}{W_H}(1-b_n^{\mathrm{WD},\mu})^j}{1-\sum_{j=0}^{W_H-1} \frac{P_c^{\mathrm{WD},\mu}}{W_H}(1-b_n^{\mathrm{WD},\mu})^j}, \qquad i = H. \end{cases} \tag{8}$$

Similarly, we may also derive the following equations according to Fig. 3:

$$\begin{cases} \pi_{0,j}^D = \sum_{m=0}^{W_0-j} \frac{\sum_{i=0}^{H} \pi_{i,0}^D b_e^{\mathrm{WD},\mu}(1-P_c^{\mathrm{WD},\mu})(1-b_n^{\mathrm{WD},\mu})^{m-1}}{W_0}, \\ \qquad\qquad 1 \le j \le W_0-1, \\ \pi_{i,j}^D = \pi_{0,0}^D \prod_{n=1}^{i} \sum_{m=0}^{W_i-j} \frac{b_e^{\mathrm{WD},\mu}P_c^{\mathrm{WD},\mu}(1-b_n^{\mathrm{WD},\mu})^{m-1}}{W_n}, \\ \qquad\qquad 1 \le i \le H, 1 \le j \le W_i. \end{cases} \tag{9}$$

Therefore, we can express all the stationary probabilities with $\pi_{0,0}^D$. By exploiting $\sum \pi_{i,j}^D = 1$, we may finally solve $\pi_{0,0}^D$ and derive all the stationary probabilities by leveraging Eqs. (8) and (9). We denote the probability of WD_μ attempting to transmit data as $\tau^{\mathrm{WD},\mu}$, which can be expressed as:

$$\tau^{\mathrm{WD},\mu} = b_e^{\mathrm{WD},\mu} \sum_{i=0}^{H} \pi_{i,0}^D, \tag{10}$$

since WD_μ only transmits when it has sufficient energy and its backoff counter has reduced to zero. Therefore, $\tau^{\mathrm{WD},\mu}$ can be calculated, when $P_c^{\mathrm{WD},\mu}$, $b_n^{\mathrm{WD},\mu}$, and $b_e^{\mathrm{WD},\mu}$ are given. Note that $b_n^{\mathrm{WD},\mu}$ and $b_e^{\mathrm{WD},\mu}$ can be obtained by solving the 1D Markov chain in the energy domain.

C. Analysis in the energy domain

According to the analysis in the data transmission domain, when the Markov chain of Fig. 3 becomes stationary, we

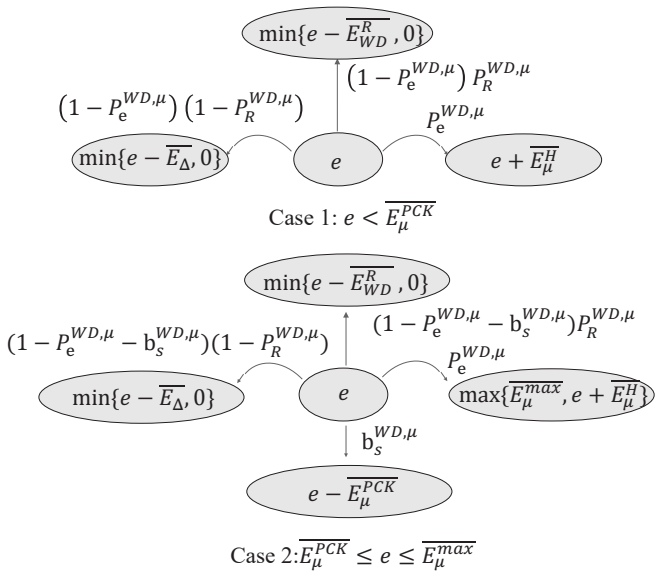

Fig. 4. 1D Markov chain in the energy domain.

can formulate the probability $b_s^{\mathrm{WD},\mu}$ of WD_μ successfully transmitting a packet as:

$$b_s^{\mathrm{WD},\mu} = (1 - P_c^{\mathrm{WD},\mu}) \sum_{i=0}^{H} \pi_{i,0}^{D} = \frac{\tau^{\mathrm{WD},\mu}(1 - P_c^{\mathrm{WD},\mu})}{b_e^{\mathrm{WD},\mu}}. \quad (11)$$

The state of WD_μ is denoted as $[e(t) = e]$ in the energy domain. Furthermore, we still assume that $\overline{E_\mu}^{\mathrm{PCK}} > \overline{E}_\Delta$ and $\overline{E_\mu}^{\mathrm{PCK}} < E_\mu^{max} - \overline{E_\mu}^{H}$. The state transitions of WD_μ's energy storage can be summarized into a Markov chain with 4 cases, as depicted in Fig. 4.

If WD_μ's energy storage is lower than $\overline{E_\mu}^{\mathrm{PCK}}$, as shown in Case 1 of Fig. 4, it does not have sufficient energy for data packet transmissions. Specifically, in Case 1 of $e < \overline{E_\mu}^{\mathrm{PCK}}$, WD_μ may harvest $\overline{E_\mu}^{H}$ energy with a probability of $P_e^{\mathrm{WD},\mu}$. WD_μ's state then transits to $[e + \overline{E_\mu}^{H}]$. Otherwise, the WD_μ may consume $\overline{E}_\Delta$ energy with a probability of $(1 - P_e^{\mathrm{WD},\mu})(1 - P_R^{\mathrm{WD},\mu})$, or it may consume $\overline{E}_{\mathrm{WD}}^{R}$ energy with a probability of $(1 - P_e^{\mathrm{WD},\mu})P_R^{\mathrm{WD},\mu}$. The energy storage of a device is lower-bounded by 0 as shown in Case 1 of Fig. 4.

If the energy storage is higher than $\overline{E_\mu}^{\mathrm{PCK}}$, as shown in Case 2 of Fig. 4, WD_μ attempts to transmit its data packets. Specifically, in Case 2 of $\overline{E_\mu}^{\mathrm{PCK}} \le e \le \overline{E_\mu}^{max}$, WD_μ may harvest $\overline{E_\mu}^{H}$ energy and its state transits to $[e + \overline{E_\mu}^{H}]$ with a probability of $P_e^{\mathrm{WD},\mu}$. Furthermore, if WD_μ successfully transmits a data packet, its energy state transits to $[e - \overline{E_\mu}^{\mathrm{PCK}}]$ with a probability of $b_s^{\mathrm{WD},\mu}$. Otherwise, WD_μ may consume $\overline{E}_\Delta$ energy for the backoff process with a probability of $(1 - b_s^{\mathrm{WD},\mu} - P_e^{\mathrm{WD},\mu})(1 - P_R^{\mathrm{WD},\mu})$, or it may consume $\overline{E}_{\mathrm{WD}}^{R}$ energy for data reception with a probability of $(1 - b_s^{\mathrm{WD},\mu} - P_e^{\mathrm{WD},\mu})P_R^{\mathrm{WD},\mu}$. Similarly, WD_μ's energy storage is upper-bounded by $\overline{E_\mu}^{max}$.

According to Fig. 4, we can further formulate the transition probabilities of all the energy states as

$$\begin{cases} P_r\{0|e\} = 1 - P_e^{\mathrm{WD},\mu}, 0 \le e < \overline{E}_\Delta, \\ P_r\{0|e\} = (1 - P_e^{\mathrm{WD},\mu})P_R^{\mathrm{WD},\mu}, \overline{E}_\Delta \le e < \overline{E}_{\mathrm{WD}}^{R}, \\ P_r\{e - \overline{E}_{\mathrm{WD}}^{R}|e\} = (1 - P_e^{\mathrm{WD},\mu})P_R^{\mathrm{WD},\mu}, \overline{E}_{\mathrm{WD}}^{R} \le e < \overline{E_\mu}^{\mathrm{PCK}}, \\ P_r\{e - \overline{E}_\Delta|e\} = (1 - P_e^{\mathrm{WD},\mu})(1 - P_R^{\mathrm{WD},\mu}), \overline{E}_\Delta \le e < \overline{E_\mu}^{\mathrm{PCK}}, \\ P_r\{e - \overline{E}_\Delta|e\} = (1 - P_e^{\mathrm{WD},\mu} - b_s^{\mathrm{WD},\mu})(1 - P_R^{\mathrm{WD},\mu}) \\ \qquad\qquad , \overline{E_\mu}^{\mathrm{PCK}} \le e \le E_\mu^{max}, \\ P_r\{e - \overline{E}_{\mathrm{WD}}^{R}|e\} = (1 - P_e^{\mathrm{WD},\mu} - b_s^{\mathrm{WD},\mu})P_R^{\mathrm{WD},\mu} \\ \qquad\qquad , \overline{E_\mu}^{\mathrm{PCK}} \le e \le E_\mu^{max}, \\ P_r\{e - \overline{E_\mu}^{\mathrm{PCK}}|e\} = b_s^{\mathrm{WD},\mu}, \overline{E_\mu}^{\mathrm{PCK}} \le e \le E_\mu^{max}, \\ P_r\{e + \overline{E_\mu}^{H}|e\} = P_e^{\mathrm{WD},\mu}, 0 \le e \le E_\mu^{max} - \overline{E_\mu}^{H}, \\ P_r\{E_\mu^{max}|e\} = P_e^{\mathrm{WD},\mu}, E_\mu^{max} - \overline{E_\mu}^{H} \le e \le E_\mu^{max}. \end{cases} \quad (12)$$

Stationary probabilities can be obtained by $\lim_{n\to\infty} \mathbf{P}^n$. Therefore, we can get the stationary probabilities of WD_μ's energy state by substituting the transition probabilities in Eq. (12) into a transition probability matrix $\mathbf{P}$, and solve the $\lim_{n\to\infty} \mathbf{P}^n$. Given the stationary probabilities, we may formulate $b_n^{\mathrm{WD},\mu}$, $b_e^{\mathrm{WD},\mu}$ and $b_r^{\mathrm{WD},\mu}$ as

$$\begin{cases} b_e^{\mathrm{WD},\mu} = \sum_{e=\overline{E_\mu}^{\mathrm{PCK}}}^{\overline{E_\mu^{max}}} \pi_e^E, \\ b_n^{\mathrm{WD},\mu} = \pi_0^E, \\ b_r^{\mathrm{WD},\mu} = \sum_{e=\overline{E}_{WD}^{\mathrm{R}}}^{\overline{E_\mu^{max}}} \pi_e^E, \end{cases} \quad (13)$$

where π_e^E represents the stationary probability of WD_μ having an energy storage of e. Note that $b_n^{\mathrm{WD},\mu}$ represents the probability of WD_μ having no energy at all. Moreover, $b_e^{\mathrm{WD},\mu}$ represents the probability of WD_μ's energy storage being higher than $\overline{E_\mu}^{\mathrm{PCK}}$.

D. Transmission probabilities and throughput analysis

The authors of [14] studied the transmission probability of a device which adopts a CSMA/CA protocol. According to its conclusion, the transmission probability is a function of its collision probability. In our system, the device adopts a similar protocol, but it may suffer from insufficient energy problem. Therefore, apart from collision probability, the device's transmission probability is also related to its energy status. However, as for the HAP, it is a device with a stable energy source. It does not suffer from any energy problems. The HAP's transmission probability is the same as [14], which is only related to the collision probability. It can be expressed as:

$$\tau^{AP} = \frac{2}{1 + W + P_c^{AP} W \sum_{i=0}^{H-1} (2P_c^{AP})^i}, \quad (14)$$

where P_c^{AP} is the collision probability of the HAP's transmission.

Given the transmission probabilities $\tau^{WD,\mu}$ of WDs and τ^{AP} of HAP, when the system is in a stationary state, we can further analyze the probability of WD_μ harvesting energy and the probabilities of WD_μ's and HAP's collisions.

The HAP can only transmit data packets successfully when there are no concurrent transmissions of all the WDs. Therefore, P_c^{AP} is expressed as:

$$P_c^{AP} = 1 - \prod_{\mu=1}^{N}(1 - \tau^{WD,\mu}). \tag{15}$$

Observe form Eq. (14) and Eq. (15), the HAP's transmission probability τ^{AP} is related to all devices' transmission probabilities.

The device's transmission collision happens when there are some transmission attempts from other devices. When WD_μ is transmitting, the probability $P_c^{WD,\mu}$ can be obtained as:

$$P_c^{WD,\mu} = 1 - (1 - \tau^{AP}) \prod_{\mu'=1,\mu'\neq\mu}^{N} (1 - \tau^{\text{WD},\mu'}). \tag{16}$$

Moreover, WD_μ can harvest energy when the HAP is transmitting to another device. By assuming that the HAP has equal probabilities to transmit data packets to all devices when the WD_μ is not transmitting packets, the probability $P_e^{WD,\mu}$ is expressed as:

$$\begin{aligned} P_e^{WD,\mu} &= \frac{(N-1/N)\tau^{AP}\prod_{\mu'=1}^{N}(1-\tau^{\text{WD},\mu'})}{(1-\tau^{\text{WD},\mu})} \\ &= \frac{N-1}{N}\tau^{AP} \prod_{\mu'=1,\mu'\neq\mu}^{N} (1 - \tau^{\text{WD},\mu'}), \end{aligned} \tag{17}$$

The WD_μ can receive a packet only when it has sufficient energy and the HAP transmit to WD_μ with no collisions. Since the HAP has equal probabilities to transmit data packets to all devices, when the WD_μ is not transmitting packets, its probability of receiving a packet from the HAP is expressed as:

$$P_R^{WD,\mu} = \frac{b_r^{\text{WD},\mu}}{N}\tau^{AP} \prod_{\mu'=1,\mu'\neq\mu}^{N} (1 - \tau^{\text{WD},\mu'}), \tag{18}$$

Algorithm 1, which has the complexity of $\mathcal{O}((\overline{E}_\mu^{max})^2 MN)$, is proposed for iteratively solving the transmission probabilities $\{\tau^{WD,\mu}\}$ of all devices, that of the HAP, as well as the probability $P_e^{\text{WD},\mu}$ of a device harvesting energy, the probability $P_R^{WD,\mu}$ of a device receiving packets and the transmission collision probabilities $P_c^{\text{WD},\mu}$ and P_c^{AP} of all devices and the HAP.

By assuming that all devices and the HAP always have packets to send, the system throughput R is formulated as

$$R = \frac{\mathbf{E}[PCK]}{\mathbf{E}[\textit{time-slot}]}, \tag{19}$$

where $\mathbf{E}[PCK]$ is the average payload length transmitted in a slot time, while $\mathbf{E}[\textit{time-slot}]$ represents the average duration of each state of the 3D Markov chain mentioned in Section III-A.

As exemplified in Fig. 1, when a transmission frame successfully delivers data packets from a source to a destination, it may have a duration expressed as

$$\begin{aligned} \text{T}_s = \text{T}_{\text{RTS}} + \text{T}_{\text{SIFS}} + \text{T}_\delta + \text{T}_{\text{CTS}} + \text{T}_{\text{SIFS}} + \text{T}_\delta + \text{T}_{\text{PCK}} \\ + \text{T}_{\text{SIFS}} + \text{T}_\delta + \text{T}_{\text{ACK}} + \text{T}_{\text{DIFS}} + \text{T}_\delta, \end{aligned} \tag{20}$$

Algorithm 1 Iterative algorithm for calculating probabilities

Input: The maximum backoff stage H; The initial backoff window size W_0; The number of WDs N; Energy threshold $\overline{E_\mu^{\text{PCK}}}$; Energy consumption unit $\overline{E}_\Delta$; Energy harvesting amount $\overline{E_\mu^H}$;

Output: All WDs transmission probabilities $\tau^{\text{WD},\mu}$, the HAP's transmission probability τ^{AP}, All WDs energy harvesting probabilities $P_e^{\text{WD},\mu}$, All WDs transmission collisions probabilities $P_c^{\text{WD},\mu}$, All WDs receiving probabilities $P_R^{\text{WD},\mu}$ and the HAP's transmission collisions probability P_c^{AP};

```
Initialize each τ^{WD,μ} within the range of (0,1), τ^{AP} with in the range of (0,1), initial iteration number n=0;
while μ < N do
    Initialize b_e^{WD,μ}, b_n^{WD,μ} and b_r^{WD,μ};
    Obtain P_c^{WD,μ}, P_R^{WD,μ} and P_e^{WD,μ} according to (16), (17) and (18);
    while n < M do
        Obtain τ^{WD,μ} and b_s^{WD,μ} according to (10) and (11);
        Obtain b_e^{WD,μ}, b_n^{WD,μ} and b_r^{WD,μ} according to (13);
        n = n + 1;
    end while
    Obtain P_c^{AP} and τ^{AP} according to (15) and (14);
    Update μ = μ + 1;
end while
return
```

where T_δ represents a constant duration of a data packet transmission in the air. However, when a transmission collision happens, a transmission frame only has a duration expressed as

$$\text{T}_c = \text{T}_{\text{RTS}} + \text{T}_{\text{DIFS}} + \text{T}_\delta, \tag{21}$$

Let P_f denote the probability of the channel being free, which indicates that neither devices nor the HAP is trying to transmit. Therefore, we can formulate P_f as

$$P_f = (1 - \tau^{AP}) \prod_{\mu'=1}^{N} (1 - \tau^{WD,\mu'}). \tag{22}$$

Let P_s^{AP} and P_s^{WD} represent the probability of the channel being occupied by a successful transmission from the HAP and a device, respectively. When the channel is occupied by a successful transmission from the HAP, no device is allowed to access the channel and the destination of the downlink packet should have sufficient energy. Therefore, the probability P_s^{AP} of the HAP occupying the channel is expressed as

$$P_s^{AP} = \sum_{\mu=1}^{N} \frac{b_r^{\text{WD},\mu}}{N}\tau^{AP} \prod_{\mu'=1}^{N} (1 - \tau^{WD,\mu'}), \tag{23}$$

Moreover, when a device occupies the channel, all the other devices and the HAP are not allowed to access the channel. The probability P_s^{WD} of the channel being occupied by a device is expressed as

$$P_s^{\text{WD}} = \sum_{\mu=1}^{N} \tau^{WD,\mu}(1 - \tau^{AP}) \prod_{\mu'=1,\mu'\neq\mu}^{N} (1 - \tau^{WD,\mu'}), \tag{24}$$

TABLE II
PARAMETER SETTING

Parameter	Value	Parameter	Value
Duration of RTS packet $\mathrm{T_{RTS}}$	288 μs	Bandwidth B	20 MHz
Duration of CTS packet $\mathrm{T_{CTS}}$	240 μs	Operation frequency f_0	2.4 GHz
Duration of ACK packet $\mathrm{T_{ACK}}$	240 μs	Maximum backoff stage H	6
Signal propagation delay T_δ	1 μs	Transmit power of the HAP	1 W
Duration of a time slot T_f	50 μs	Antenna gains G_R G_T	6 dBi
Duration of SIFS $\mathrm{T_{SIFS}}$	28 μs	Length of PCK L[PCK]	8 Kb
Duration of DIFS $\mathrm{T_{DIFS}}$	128 μs	Transmission bit rate	1 Mbps
Initial backoff window size W_0	16	Supercapacitor's maximum capacity Q	1 J (5 V 80 mF)

As a result, the total probability of the channel being occupied is obtained as

$$P_s = \sum_{\mu=1}^{N} \frac{b_r^{\mathrm{WD},\mu}}{N} \tau^{AP} \prod_{\mu'=1}^{N} (1-\tau^{WD,\mu'}) + \sum_{\mu=1}^{N} \tau^{WD,\mu}(1-\tau^{AP}) \prod_{\mu'=1,\mu'\neq\mu}^{N} (1-\tau^{WD,\mu'}). \tag{25}$$

Eventually, the average length of a slot time can be formulated as

$$\mathbf{E}[\textit{time-slot}] = P_f \mathrm{T}_f + P_s \mathrm{T}_s + (1-P_f-P_s)\mathrm{T}_c, \tag{26}$$

where the T_f is the duration of an empty slot time.

Furthermore, we assume that each data packet has a fixed length of L[PCK]. The average payload can be formulated as

$$\mathbf{E}[PCK] = \underbrace{P_s^{AP} L[\mathrm{PCK}]}_{downlink} + \underbrace{P_s^{\mathrm{WD}} L[\mathrm{PCK}]}_{uplink}. \tag{27}$$

Based on Eqs. (19) and (26), both the downlink and the uplink throughputs are expressed as

$$\begin{cases} R_{downlink} = \frac{P_s^{AP} L[\mathrm{PCK}]}{P_f \mathrm{T}_f + P_s \mathrm{T}_s + (1-P_f-P_s)\mathrm{T}_c}, \\ R_{uplink} = \frac{P_s^{\mathrm{WD}} L[\mathrm{PCK}]}{P_f \mathrm{T}_f + P_s \mathrm{T}_s + (1-P_f-P_s)\mathrm{T}_c}, \end{cases} \tag{28}$$

In our system, only the HAP is powered by a stable energy source, while the devices are recharged by the HAP's downlink transmissions. Therefore, the total power consumed by the whole network is from the HAP. With all the probabilities derived above, the average power consumed by the HAP can be analyzed. When the channel is occupied by the HAP, it transmits packets in the downlink with a power of P_{AP}. When the channel is occupied by a device, the HAP receives packets in the uplink. Its energy consumption is E_{AP}^R. Therefore, the average power consumed by the HAP can be expressed as:

$$P_{Totol} = \frac{P_s^{AP} P_{AP} \mathrm{T_{PCK}} + P_s^{\mathrm{WD}} E_{AP}^R + (1-P_s) E_\Delta}{P_f \mathrm{T}_f + P_s \mathrm{T}_s + (1-P_f-P_s)\mathrm{T}_c}. \tag{29}$$

IV. SIMULATION RESULTS

Without specific statements, all parameters in our simulation are provided in TABLE II. The MAC layer parameters are from the IEEE 802.11 standard [32]. The transmit power of the HAP is set to 1 W, while the antennas' gain is set to 6 dBi. The maximum capacity of the device's supercapacitor is 1 J [33].

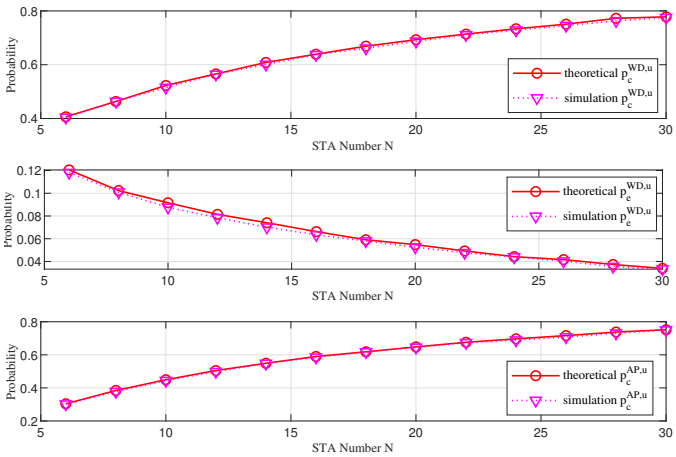

Fig. 5. Probabilities versus the number of wireless devices, where H=4,W=8,$E_\mu^{\max}$=1000 and $\overline{E}_\Delta$=1

First of all, our theoretical analysis on $P_c^{WD,\mu}$, P_c^{AP} and $P_e^{WD,\mu}$ by using Algorithm 1 are validated by Monte-Carlo simulation in Fig. 5. Both the transmission collision probability of a device and that of the HAP increase as we increase the number of devices. This is because more devices may compete to access the channel for their own transmissions. By contrast, the energy harvesting probability decreases as the number of devices increases. This is because the HAP may gain fewer opportunities to facilitate its downlink transmissions, which reduces the energy harvesting opportunities for the devices.

Observe from Fig. 6 that $P_e^{WD,\mu}$, $P_c^{WD,\mu}$, τ^{AP} and $\tau^{\mathrm{WD},\mu}$ all reduces as we increase the initial window size W_0. Specifically, both the transmission collision probabilities τ^{AP} and $\tau^{\mathrm{WD},\mu}$ decrease because an increasing W_0 prolongs the backoff process of the devices and the HAP, which reduces their opportunities of data packet transmissions. Observe from Fig. 6 that reducing τ^{AP} may let devices gain more opportunities to access the channel, which then increases their transmission probabilities $\tau^{WD,\mu}$. However, further reducing τ^{AP} may also reduce the energy harvesting probability $P_e^{WD,\mu}$ of devices. Since the amount of energy harvested is reduced, the transmission probability $\tau^{\mathrm{WD},\mu}$ of devices may further reduce. Moreover, with an increasing initial window size W_0, concurrent transmissions can be substantially avoided. Therefore, the transmission collision probabilities $P_c^{\mathrm{WD},\mu}$ and

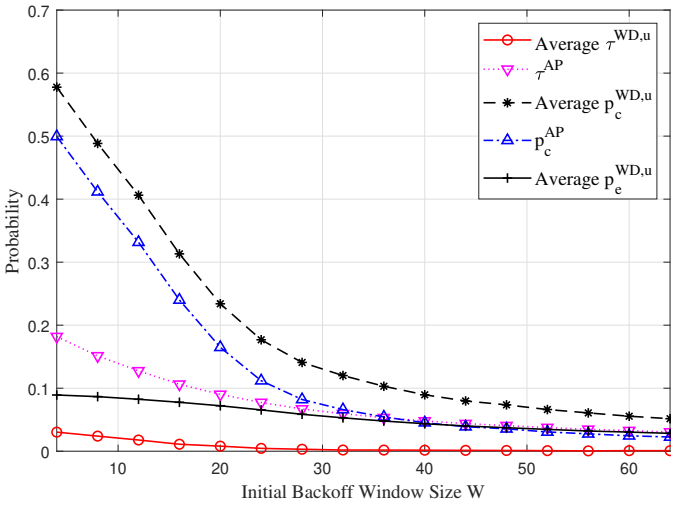

Fig. 6. Probabilities versus initial backoff window size W_0, where H=4,W=8,N=20 and $\overline{E}_\Delta$=1

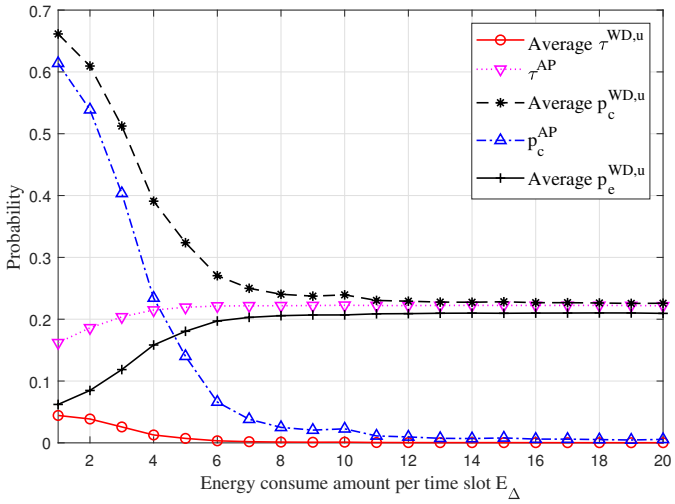

Fig. 7. Probabilities versus $\overline{E}_\Delta$, where H=4,W=8,N=20

P_c^{AP} both reduces. Note that Algorithm 1 helps us to obtain all devices' transmission probabilities $\{\tau^{\text{WD},\mu}\}$ and transmission collision probabilities $\{P_c^{\text{WD},\mu}\}$ and P_c^{AP}. These probabilities have similar trends. For clarity, we plot the average value of all these probabilities among all devices in Fig. 6. Similar approach is adopted in the rest of this section.

We study the impact of the energy consumption $\overline{E}_\Delta$ for backoff operation on both the transmission probabilities and collision probabilities of the devices and the HAP in Fig. 7. Observe from Fig. 7 that as we increase $\overline{E}_\Delta$, the device's transmission probability $\tau^{\text{WD},\mu}$, the HAP's collision probability P_c^{AP} and the device's collision probability $P_c^{WD,\mu}$ all reduce and converge to a certain value. By contrast, the HAP's transmission probability τ^{AP} and the device's energy harvesting probability $P_e^{WD,\mu}$ both increase and converge to a certain value, as we increase $\overline{E}_\Delta$. This is because, with an increasing $\overline{E}_\Delta$, a device may quickly run out of its energy storage during the backoff and the packet exchange process. Therefore, it may not have sufficient energy to transmit any data packets, which results in the reduction of the transmission probability $\tau^{\text{WD},\mu}$. As $\tau^{\text{WD},\mu}$ decreases, the HAP gains more opportunity to transmit its own data packets in the downlink, since it is not constrained by the energy storage. Therefore, its transmission probability τ^{AP} increases, while its collision probability reduces. Moreover, frequent downlink transmissions of the HAP indicate that the devices have an increasing chance of harvesting energy, which results in an increasing energy harvesting probability $P_e^{WD,\mu}$. However, when $\overline{E}_\Delta$ becomes higher than the energy E_μ^H harvested by a device, it may not have any remaining energy storage to power the data transmissions, since all the energy harvested is consumed for the backoff and packet exchange process. As a result, we only have the HAP to transmit data packets in the system. Therefore, all these probabilities finally converge to a constant value.

Given all these transmission probabilities and collision probabilities, we may evaluate the throughput performance of the system, according to Eq. (26). Therefore, both the downlink and the uplink throughput are portrayed in Fig. 8. Interestingly, the total uplink throughput does not always increase as we increase the number N of the devices. This is because, with more devices, the channel is more efficiently used for data packet transmissions, which results in increasing uplink throughput. However, when the number of devices continuously increases, transmission collisions may frequently happen, which then reduces the uplink throughput. Moreover, observe from Fig. 8 (a) that when we have fewer devices, a higher $\overline{E}_\Delta$ may result in a lower uplink throughput. This is because a higher energy consumption for packet exchange and backoff process may reduce the energy consumption for data transmissions. By contrast, when we have a higher number of devices, an increasing $\overline{E}_\Delta$ reduces the collision probability $P_c^{WD,\mu}$, which may increase the total uplink throughput. Observe from Fig. 8 (b) that, as we increase the total number of devices, the downlink throughput of the HAP reduces all the time. This is because when more devices compete for data packet transmissions, the collision probability P_c^{AP} of the HAP increases, which thus reduces the downlink throughput. However, when $\overline{E}_\Delta$ increases, the devices do not have sufficient energy to support their own data packet transmissions. Therefore, the HAP may gain more opportunities to increase its downlink throughput.

In Fig. 9, we investigate the total throughput with different duration T_{PCK}. As we increase T_{PCK}, the total throughput firstly increases. This is because once the downlink transmission of the HAP commences, devices may harvest more energy for powering their data packet transmissions. However, as we continuously increase T_{PCK}, all devices may occupy the channel for a longer time, which thus increases the transmission collision probabilities. Therefore, the total throughput reduces. Furthermore, a higher number of devices may increase their collision probabilities, which then decrease P_s^{WD} and P_s^{AP} in Eq. (26). Therefore, the total throughput reduces.

In Fig. 10, we investigate the impact of the initial backoff window size W_0 and the maximum backoff stage H on the throughput performance. As we increase the initial backoff

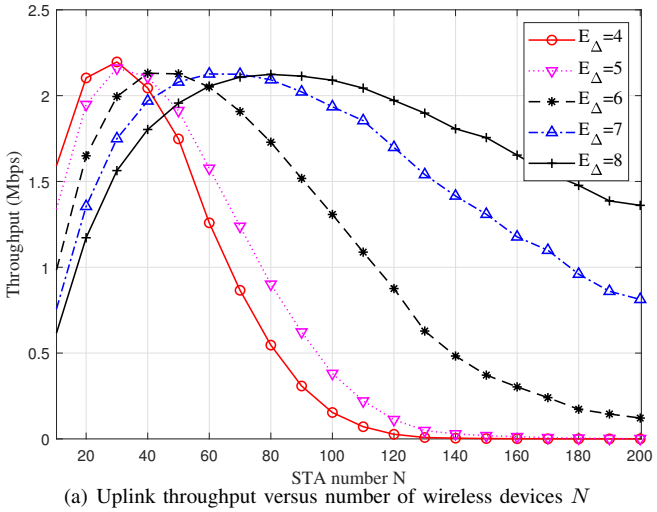

(a) Uplink throughput versus number of wireless devices N

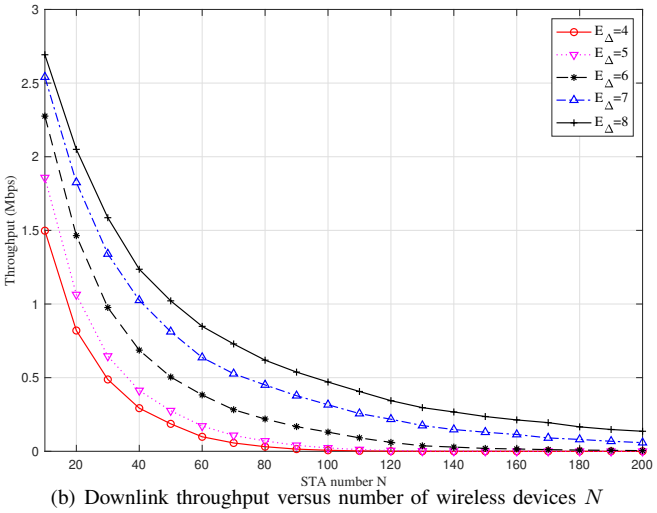

(b) Downlink throughput versus number of wireless devices N

Fig. 8. Uplink throughput and downlink throughput versus number of wireless devices N, where H=4 and W=8

window size W, it reduces the HAP's transmission collision probability at first, which then increases the downlink throughput. However, as we continuously increase W, the HAP's downlink throughput reduces. Moreover, A higher W also reduces $\tau^{\mathrm{WD},\mu}$, which results in a decreasing uplink throughput. Similarly, the maximum backoff stage H may substantially prolong the backoff process. Therefore, an increasing H may increase the downlink throughput and decrease the uplink throughput, as shown in Fig. 10.

In Fig. 11, we study the impact of duration $\mathrm{T_{PCK}}$ on the power consumption of the HAP. By increasing $\mathrm{T_{PCK}}$, the power consumption increases. This is because the HAP may consume more power to transmit downlink packets as $\mathrm{T_{PCK}}$ increases. With the increasing $\mathrm{T_{PCK}}$, devices further harvest more energy, and devices may get more opportunities to occupy the channel and P_s^{WD} may much larger than P_s^{AP} when $\mathrm{T_{PCK}}$ is sufficiently long. In this situation, the impact of $\mathrm{T_{PCK}}$ on the energy consumption is trivial, since the $\mathrm{T_{PCK}}$ is only related to the P_s^{AP} in Eq. (28). Moreover, by increasing the number of devices, the power consumption of the HAP decreases. This is because with the increasing number of devices, all

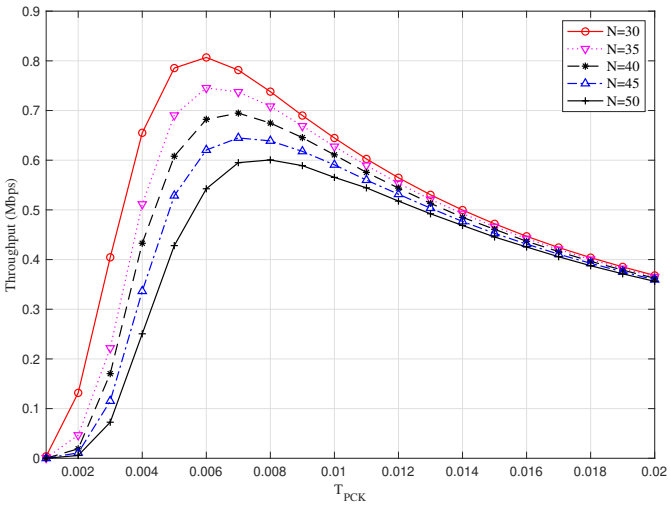

Fig. 9. Total throughput versus duration of a successful transmission $\mathrm{T_{PCK}}$, where H=4,W=8 and $\overline{E}_{\Delta}$=4

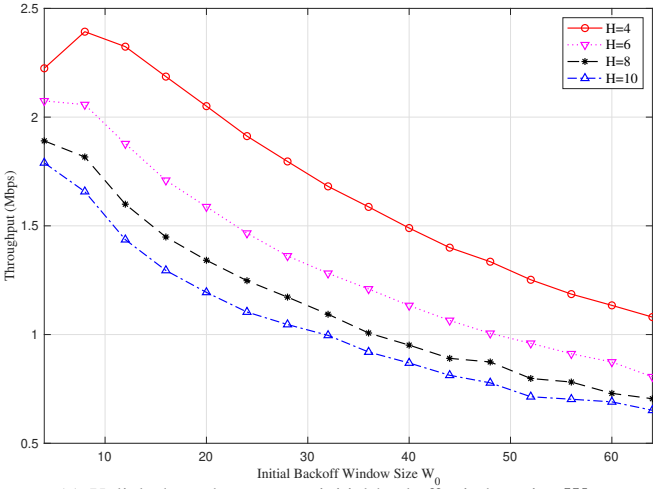

(a) Uplink throughput versus initial backoff window size W_0

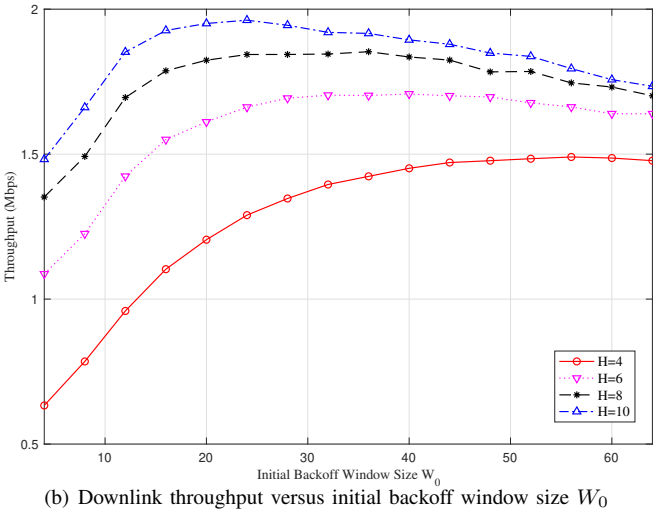

(b) Downlink throughput versus initial backoff window size W_0

Fig. 10. Uplink throughput and downlink throughput versus initial backoff window size W_0, where N=15 and $\overline{E}_{\Delta}$=4

devices suffer from more collisions, and the HAP thus takes more backoff operations than packet receptions. Therefore, the system consumes less energy.

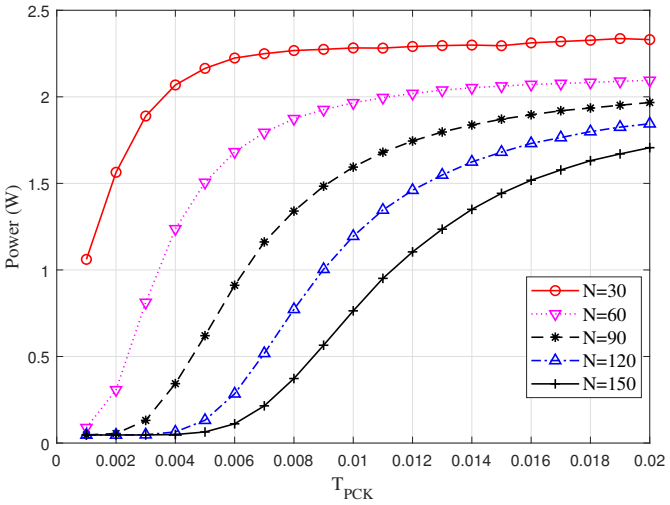

Fig. 11. Energy consumed by HAP versus duration of a successful transmission T_{PCK}, where H=4,W=8,$\overline{E}_{\Delta}$=4 and $P_{AP} = 1W$

V. Conclusion

In this paper, a 3D Markov chain is exploited for characterizing the data transmission, energy harvesting, and energy consumption patterns of all the batteryless wireless devices and the HAP. A decoupling method is adopted for obtaining a semi-closed-form analysis of various transmission probabilities and throughput. The Monte-Carlo simulation validates the accuracy of our theoretical modeling. Moreover, both the simulation and theoretical results demonstrate that the uplink throughput does not always increase when we have more wireless devices. Increasing the initial backoff window size also reduces the uplink throughput. Our theoretical modeling provides an effective and fast way to study the performance of batteryless access with a distributed collision avoidance protocol. Specifically, according to our parameters set, the average energy consumption $\overline{E}_{\Delta}$ of the batteryless device should not be larger than 5 mJ/s when there are 20 WDs in a DEIN system. Moreover, the data packet transmission duration can be set to 6 ms to achieve the best throughput performance. Furthermore, the initial backoff window size W_0 should be carefully chosen in a system with N devices in order to maximize the throughput performance.

References

[1] X. Lu, P. Wang, D. Niyato, D. I. Kim, and Z. Han, "Wireless Networks With RF Energy Harvesting: A Contemporary Survey," *IEEE Commun. Surveys Tuts.*, vol. 17, no. 2, pp. 757–789, 2015.

[2] A. Padhy, S. Joshi, S. Bitragunta, V. Chamola, and B. Sikdar, "A Survey of Energy and Spectrum Harvesting Technologies and Protocols for Next Generation Wireless Networks," *IEEE Access*, vol. 9, pp. 1737–1769, 2021.

[3] D. Ma, G. Lan, M. Hassan, W. Hu, and S. K. Das, "Sensing, Computing, and Communications for Energy Harvesting IoTs: A Survey," *IEEE Commun. Surveys Tuts.*, vol. 22, no. 2, pp. 1222–1250, 2020.

[4] O. B. Akan, O. Cetinkaya, C. Koca, and M. Ozger, "Internet of Hybrid Energy Harvesting Things," *IEEE Internet Things J.*, vol. 5, no. 2, pp. 736–746, 2018.

[5] T. Ruan, Z. J. Chew, and M. Zhu, "Energy-Aware Approaches for Energy Harvesting Powered Wireless Sensor Nodes," *IEEE Sensors J.*, vol. 17, no. 7, pp. 2165–2173, 2017.

[6] M.-L. Ku, W. Li, Y. Chen, and K. J. Ray Liu, "Advances in Energy Harvesting Communications: Past, Present, and Future Challenges," *IEEE Commun. Surveys Tuts.*, vol. 18, no. 2, pp. 1384–1412, 2016.

[7] J. Hu, K. Yang, G. Wen, and L. Hanzo, "Integrated Data and Energy Communication Network: A Comprehensive Survey," *IEEE Commun. Surveys Tuts.*, vol. 20, no. 4, pp. 3169–3219, 2018.

[8] J. Hu, Q. Wang, and K. Yang, "Energy Self-Sustainability in Full-Spectrum 6G," *IEEE Wireless Commun.*, vol. 28, no. 1, pp. 104–111, 2021.

[9] K. Yang, Q. Yu, S. Leng, B. Fan, and F. Wu, "Data and Energy Integrated Communication Networks for Wireless Big Data," *IEEE Access*, vol. 4, pp. 713–723, 2016.

[10] Y. Huang and B. Clerckx, "Waveform design for wireless power transfer with limited feedback," *IEEE Transactions on Wireless Communications*, vol. 17, no. 1, pp. 415–429, 2018.

[11] X. Lu, I. Flint, D. Niyato, N. Privault, and P. Wang, "Self-Sustainable Communications With RF Energy Harvesting: Ginibre Point Process Modeling and Analysis," *IEEE J. Sel. Areas Commun.*, vol. 34, no. 5, pp. 1518–1535, 2016.

[12] C.-H. Liu and C.-S. Hsu, "Fundamentals of Simultaneous Wireless Information and Power Transmission in Heterogeneous Networks: A Cell-Load Perspective," *IEEE J. Sel. Areas Commun.*, vol. 37, no. 1, pp. 100–115, 2019.

[13] S. Guruacharya and E. Hossain, "Self-sustainability of energy harvesting systems: Concept, analysis, and design," *IEEE Transactions on Green Communications and Networking*, vol. 2, no. 1, pp. 175–192, 2018.

[14] G. Bianchi, "Performance analysis of the IEEE 802.11 distributed coordination function," *IEEE J. Sel. Areas Commun.*, vol. 18, no. 3, pp. 535–547, 2000.

[15] Z. Chen, L. X. Cai, Y. Cheng, and H. Shan, "Sustainable cooperative communication in wireless powered networks with energy harvesting relay," *IEEE Transactions on Wireless Communications*, vol. 16, no. 12, pp. 8175–8189, 2017.

[16] J. Gao, W. Zhuang, M. Li, X. Shen, and X. Li, "Mac for machine-type communications in industrial iot—part i: Protocol design and analysis," *IEEE Internet of Things Journal*, vol. 8, no. 12, pp. 9945–9957, 2021.

[17] L. Liang, X. Liu, Y. Wang, W. Feng, and G. Yang, "Sw-mac: A low-latency mac protocol with adaptive sleeping for wireless sensor networks," *WIRELESS PERSONAL COMMUNICATIONS*, vol. 77, pp. 1191–1211, JUL 2014.

[18] Z. A. Eu and H.-P. Tan, "Probabilistic polling for multi-hop energy harvesting wireless sensor networks," in *2012 IEEE International Conference on Communications (ICC)*, pp. 271–275, 2012.

[19] B. Li, X. Guo, R. Zhang, X. Du, and M. Guizani, "Performance Analysis and Optimization for the MAC Protocol in UAV-Based IoT Network," *IEEE Trans. Veh. Technol.*, vol. 69, no. 8, pp. 8925–8937, 2020.

[20] X. Guo, B. Li, and K. Liu, "Performance Analysis for the CMSA/CA Protocol in UAV-based IoT network," in *2020 IEEE 91st Vehicular Technology Conference (VTC2020-Spring)*, pp. 1–6, 2020.

[21] Y. Li, B. Cao, L. Liang, D. Mao, and L. Zhang, "Block Access Control in Wireless Blockchain Network: Design, Modeling and Analysis," *IEEE Trans. Veh. Technol.*, vol. 70, no. 9, pp. 9258–9272, 2021.

[22] J. Choi, S. Byeon, S. Choi, and K. B. Lee, "Activity Probability-Based Performance Analysis and Contention Control for IEEE 802.11 WLANs," *IEEE Trans. Mobile Comput.*, vol. 16, no. 7, pp. 1802–1814, 2017.

[23] M. Y. Naderi, P. Nintanavongsa, and K. R. Chowdhury, "Rf-mac: A medium access control protocol for re-chargeable sensor networks powered by wireless energy harvesting," *IEEE Transactions on Wireless Communications*, vol. 13, no. 7, pp. 3926–3937, 2014.

[24] P. Tamilarasi and B. Lavenya, "Energy and throughput enhancement in wireless powered communication networks using rf-mac and csma," in *2015 International Conference on Innovations in Information, Embedded and Communication Systems (ICIIECS)*, pp. 1–4, 2015.

[25] A. Iqbal, Y. Kim, and T.-J. Lee, "Access Mechanism in Wireless Powered Communication Networks With Harvesting Access Point," *IEEE Access*, vol. 6, pp. 37556–37567, 2018.

[26] S. Khairy, M. Han, L. X. Cai, and Y. Cheng, "Sustainable Wireless IoT Networks With RF Energy Charging Over Wi-Fi (CoWiFi)," *IEEE Internet Things J.*, vol. 6, no. 6, pp. 10205–10218, 2019.

[27] K. Moon, K. M. Kim, Y. Kim, and T.-J. Lee, "Device-Selective Energy Request in RF Energy-Harvesting Networks," *IEEE Commun. Lett.*, vol. 25, no. 5, pp. 1716–1719, 2021.

[28] Y. Zhao, J. Hu, Y. Diao, Q. Yu, and K. Yang, "Modelling and Performance Analysis of Wireless LAN Enabled by RF Energy Transfer," *IEEE Trans. Commun.*, vol. 66, no. 11, pp. 5756–5772, 2018.
[29] J. Lyu and R. Zhang, "Spatial throughput characterization for intelligent reflecting surface aided multiuser system," *IEEE Wireless Communications Letters*, vol. 9, no. 6, pp. 834–838, 2020.
[30] S. Wang, M. Xia, K. Huang, and Y.-C. Wu, "Wirelessly Powered Two-Way Communication With Nonlinear Energy Harvesting Model: Rate Regions Under Fixed and Mobile Relay," *IEEE Trans. Wireless Commun.*, vol. 16, no. 12, pp. 8190–8204, 2017.
[31] E. Boshkovska, D. W. K. Ng, N. Zlatanov, and R. Schober, "Practical Non-Linear Energy Harvesting Model and Resource Allocation for SWIPT Systems," *IEEE Commun. Lett.*, vol. 19, no. 12, pp. 2082–2085, 2015.
[32] "IEEE Standard for Information technology–Telecommunications and information exchange between systems Local and metropolitan area networks–Specific requirements Part 11: Wireless LAN Medium Access Control (MAC) and Physical Layer (PHY) Specifications," *IEEE Std 802.11-2012 (Revision of IEEE Std 802.11-2007)*, pp. 1–2793, 2012.
[33] Y. Zheng, Y. Zhang, Y. Wang, J. Hu, and K. Yang, "Create your own data and energy integrated communication network: A brief tutorial and a prototype system," *China Communications*, vol. 17, no. 9, pp. 193–209, 2020.

Xinyu Fan received the B.Eng. degree from North China Electric Power University, in 2019. He is now pursuing Ph.D. degree with the School of Information and Communication Engineering, University of Electronic Science and Technology of China. His current research interests include data and energy integrated networks (DEIN), batteryless access protocol and energy self-sustainable networks.

Jie Hu (S'11, M'16, SM'21) received his B.Eng. and M.Sc. degrees from Beijing University of Posts and Telecommunications, China, in 2008 and 2011, respectively, and received the Ph.D. degree from the School of Electronics and Computer Science, University of Southampton, U.K., in 2015. Since March 2016, he has been working with the School of Information and Communication Engineering, University of Electronic Science and Technology of China (UESTC). He is now a Research Professor and PhD supervisor. He won UESTC's Academic Young Talent Award in 2019. Now he is supported by the "100 Talents" program of UESTC. He is an editor for *IEEE Wireless Communications Letters*, *IEEE/CIC China Communications* and *IET Smart Cities*. He serves for *IEEE Communications Magazine*, *Frontiers in Communications and Networks* as well as *ZTE communications* as a guest editor. He is a technical committee member of ZTE Technology. He is a program vice-chair for IEEE TrustCom 2020, a technical program committee (TPC) chair for IEEE UCET 2021 and a program vice-chair for UbiSec 2022. He also serves as a TPC member for several prestigious IEEE conferences, such as IEEE Globecom/ICC/WCSP and etc. He has won the best paper award of IEEE SustainCom 2020 and the best paper award of IEEE MMTC 2021. His current research focuses on wireless communications and resource management for B5G/6G, wireless information and power transfer as well as integrated communication, computing and sensing.

Yizhe Zhao (S'16-M'21) received the PhD in information and communication engineering from University of Electronic Science and Technology of China (UESTC) in 2021, where he is currently a postdoctoral researcher. He has been a Visiting Researcher with the Department of Electrical and Computer Engineering, University of California, Davis, USA. He serves for China Communications as the guest editor of the special issue "Energy Self-Sustainability in 6G". He is also a TPC member of several prestigious IEEE conferences, such as IEEE ICC and IEEE Globecom. He manages research projects funded by National Natural Science Foundation of China (NSFC) and China Postdoctoral Science Foundation. His research interests include modulation and coding design, wireless information and power transfer, joint communication and control.

Kun Yang (M'00, SM'08, F'23) received his PhD from the Department of Electronic & Electrical Engineering of University College London (UCL), UK. He is currently a Chair Professor in the School of Computer Science & Electronic Engineering, University of Essex, leading the Network Convergence Laboratory (NCL), UK. He is also an affiliated professor at UESTC, China. Before joining in the University of Essex at 2003, he worked at UCL on several European Union (EU) research projects for several years. His main research interests include wireless networks and communications, IoT networking, data and energy integrated networks and mobile computing. He manages research projects funded by various sources such as UK EPSRC, EU FP7/H2020 and industries. He has published 400+ papers and filed 30 patents. He serves on the editorial boards of both IEEE (e.g., IEEE TNSE, IEEE ComMag, IEEE WCL) and non-IEEE journals (e.g., Deputy EiC of IET Smart Cities). He was an IEEE ComSoc Distinguished Lecturer (2020-2021). He is a Member of Academia Europaea (MAE), a Fellow of IEEE, a Fellow of IET and a Distinguished Member of ACM.